CHAPTER–3C

Effect of Molecular Geometry and Supramolecular Assembling in Bis(pyridyl)-disulfonamides on their Photophysical Properties

Effect of Molecular Geometry and Supramolecular Assembling in Bis(pyridyl)-disulfonamides on their Photophysical Properties

3C.1 Introduction

Molecular synthons capable of generating varied non-covalent interactions may lead to diverse supramolecular arrangements, which in turn will affect properties associated with molecules including photophysical properties. Presence of different functional groups in a molecular synthon will lead to a wide range of possibilities for non-covalent interactions and hence predicting the actual supramolecular arrangement of such molecules is a challenging task. The supramolecular arrangement is governed by various factors including the attainment of a stable molecular geometry by utilizing all possible non-covalent interactions. In Chapter 3A, the photophysical properties of bis(pyridyl)-di-imines were evaluated with the help of non-covalent C-H···N and π•••π interactions, while chapter 3B dealt with the assembling of pyrene based molecular systems via π•••π and C-H hydrogen bonding and resulted in N-H•••N interactions.[2d] Sulfonamides have also showed the π interactions resulting in interesting photophysical properties. Amide functional groups are studied extensively by different researcher groups to understand the possible supramolecular assemblies.[4] Efficacy of amide functional group in forming strong hydrogen bonding interactions has provided ample opportunity to molecules in forming diverse range of architectures. Presence of heteroatoms/functional groups along with amides enhances the possibilities of heteromeric synthons resulting in further diversified network architectures. One such category of molecules is bis(pyridyl)-diamides, where in some cases heteromeric synthons has resulted due to the presence of pyridyl groups, while in some molecules self-complimentary amide-to-amide hydrogen bonds are intact.[2b] Homomeric synthons formed due to self-complementary amide-to-amide hydrogen bonds between amide functional groups can be categorized as (i) α-sheets, (ii) β-sheets and (iii) (4,4)-networks. Steric constraints are mainly responsible for the interferences in these homomeric synthons[2a-c] but in the case of bis(pyridyl)-diamides, interference of amide-to-amide hydrogen bond is due to the formation of N-H•••N hydrogen bond interactions between amide NH and pyridyl nitrogen (Scheme 3C.1).[2a, b] An important analogue of amide is sulfonamide, where carbonyl (C=O) group is replaced by sulfonyl (O=S=O) group. Geometrical and electronic differences associated with the sulfur and carbon centres can be analysed by observing the synthons containing these functional groups. When no other functional groups are present in the synthon, formation of N-H•••OSO hydrogen bonding is observed.[5] Whereas, the presence of pyridyl ring interfered the self-recognition of

hydrogen bonding and resulted in N-H•••N interactions.[2d] Sulfonamides have also showed the ability to act as anion receptors.[1b] Figure 3C.1a represents the sulfonamide hydrogen bonding in host molecule which provided shape-selective anion recognition for guest molecules. Figure 3C.1b represents chiral macrocyclic multi anion receptor formed by sulfonamides.[1a]

Sulfonamides and their derivatives are used in medicinal chemistry[6] in pharmacological applications[7]. The combination of pyridyl group and sulfonamide has shown the potential

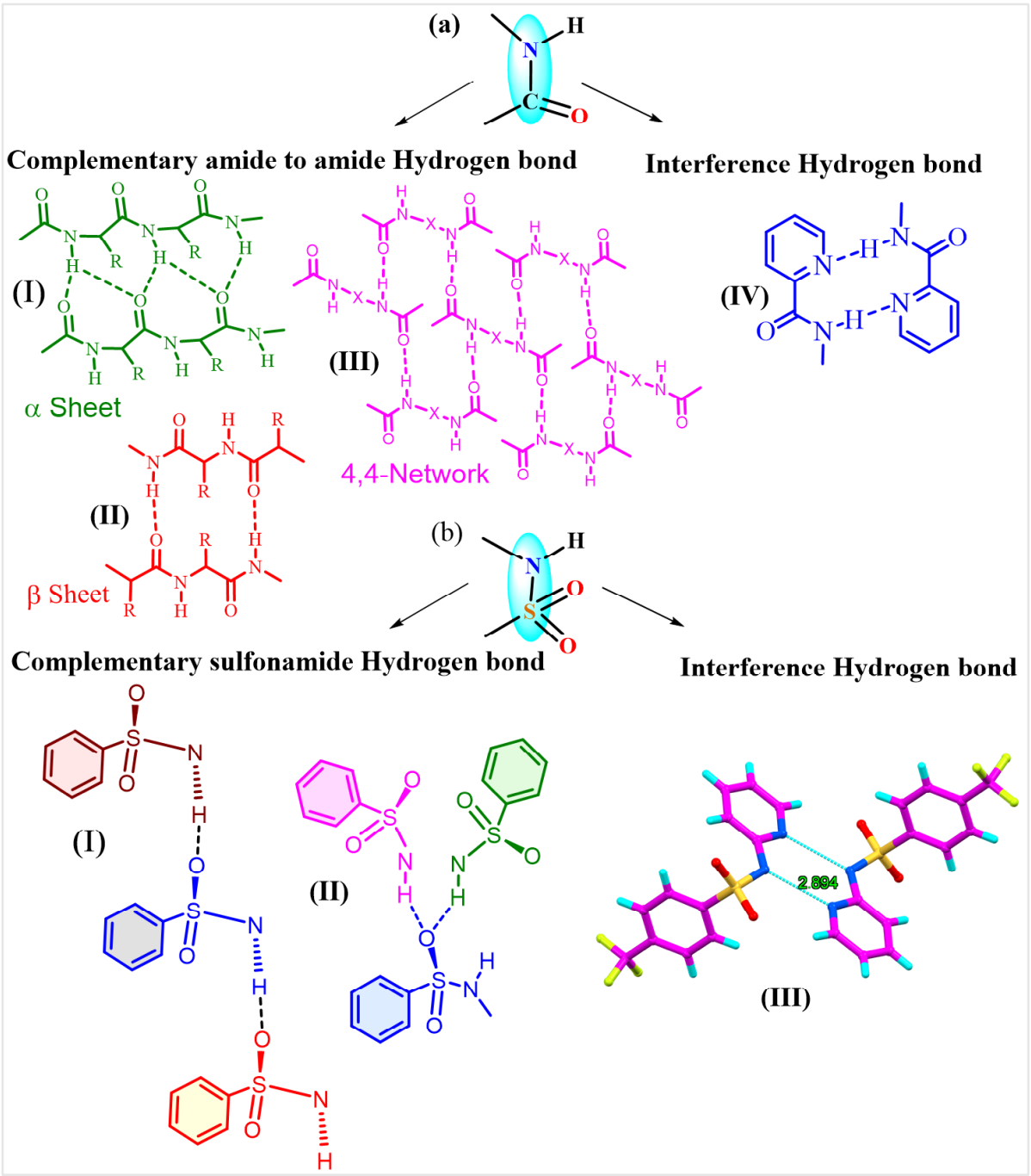

Scheme 3C.1: Various types of H-bonding synthon of amide[2]

antimicrobial activity mainly due to the electronic effects as a result of continuous conjugation of >NH-SO_2 with pyridyl ring.[8] One of the examples of sulfonamides in medicinal chemistry is phenolsulfonamides, which has been screened as chemotherapeutic agents. Sulfonamides are also used as chiral isosteres synthon for directional interactions, which are very crucial in development of pharmaceutical and agrochemical products.[9]

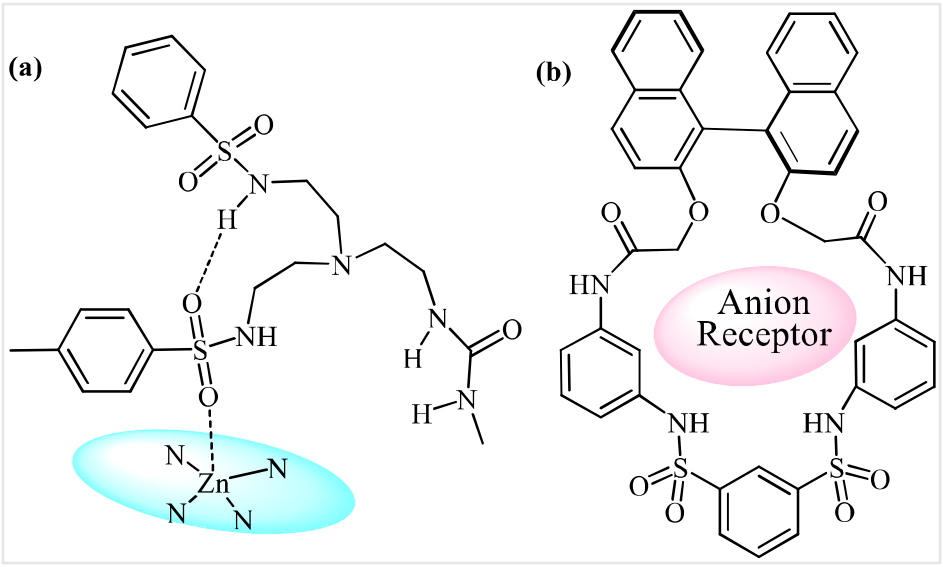

Figure 3C.1: Sulfonamide featuring as anion receptors[1]

Aggregation induced enhanced emission (AIEE) is generally observed in molecular systems where non-planarity is achieved due to the presence of multiple aryl rings which prevent aromatic π•••π stacking. Locked arrangements of molecules unique packing resulting in restricted intramolecular rotation leads to AIEE. Phenyl derivatives such as 1,2,3,4-tetraphenyl and 1,2,3,4,5-pentaphenyl benzene show AIEE.[10] In these compounds, unique molecular packing resulted in AIEE in their aggregate states. The intermolecular hydrogen bonding interactions in 2,7-bis(4-(*tert*-butylthio)-phenyl)fluorenone leads the dimer formation in the ground state and it turned into highly induce excimer in the excited state which resulted in AIE.[11] In higher concentration, the assembling of molecules is resulted in H-aggregates or J-aggregates (Scheme 3C.2).

In chapter 3B, the various possible reasons of AIE and ways to overcome ACQ problems were discussed. The aggregation caused quenching (ACQ) is the opposite phenomena of AIE. ACQ is mainly originated due to short-range aromatic interactions (3.4 Å -3.9 Å)[12] between the molecules in aggregation such as π•••π stacking which is arising from the planarity of molecular arrangement that lead the molecules to go through non-radiative relaxation pathway. Intramolecular free rotation can also dissipate the energy via non-radiative pathway in solution

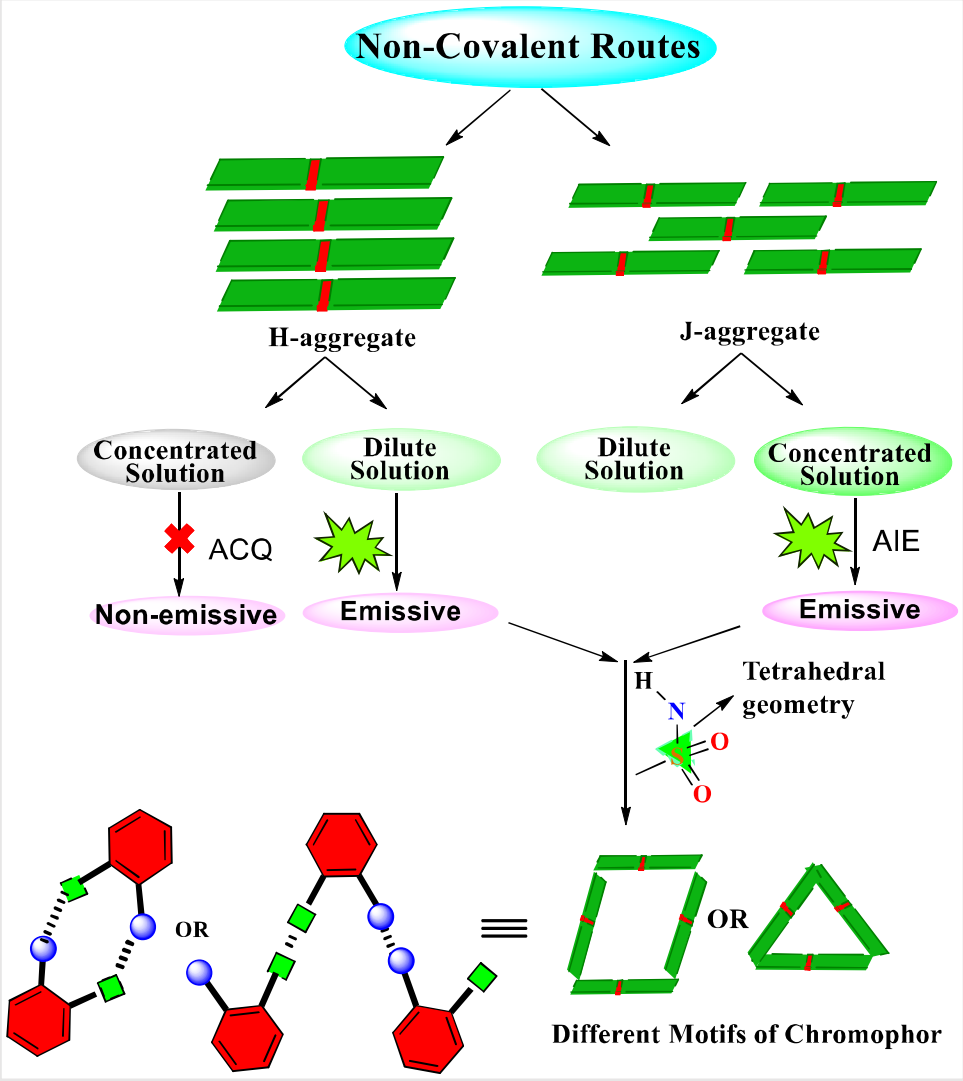

Scheme 3C.2: Schematic correlation between the non-covalent interactions and emission properties

state, but in aggregate states this dissipation is diminished due to restrictions in rotational and vibrational motions of molecules due to steric hinderance effect such as intramolecular planarization, formation of J-aggregates, intramolecular charge transfer, twisted geometry. Formation of such specific molecular arrangement can result due to various possible interactions and arrangements, where non-covalent interaction being the most important of them, which can fix the molecule at particular arrangement.

Sulfonamides tuned with different substituent groups are reported to show photophysical properties.[13]Photophysical properties of bezenesulfonamide (bzs) derivatives are explored by tuning the substituent group. The series of bzs derivatives was synthesised by Ebru Bozkart and co-worker by incorporating electron withdrawing and donating substituents in 1-phenyl group of 4-(2-(1-phenylethylidene)hydrazine) (red circle in Figure 3C.2a).[14] The derivatives of azo-sulfonamide are studied by M.S. Zakerhamidi and coworkers for the photophysical

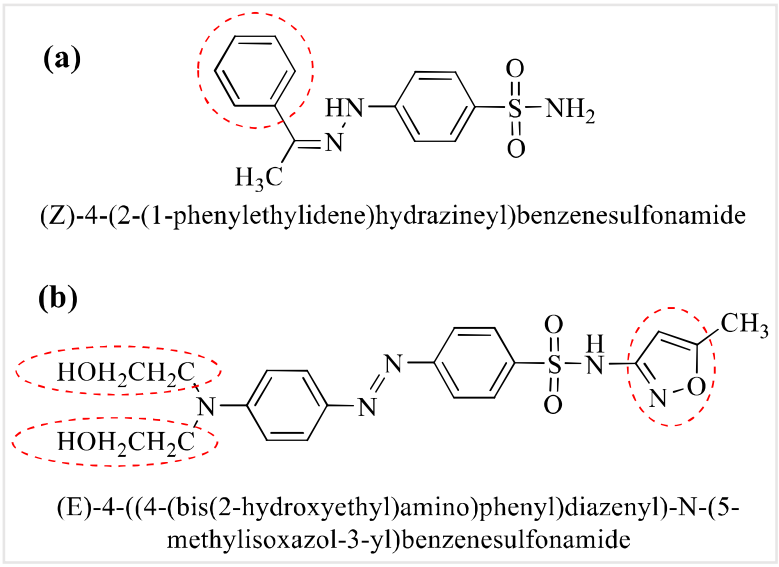

Figure 3C.2: Benzenesulfonamides tuned with various substituents to extract photophysical properties [12-13]

properties and solute-solvent interaction was observed in different solvents (red circle in Figure 3C.2b).[15] These types of sulfonamides have large and permanent dipole moment which is also varied by the presence of different substituents which in turn affects the ground state, excited electronic states and the overall photophysical process.

Crystal structure analysis[16] gives detailed structural information about the solid-state packing of the molecules. Supramolecular arrangement of molecules and interactions[17] present between them decides the photophysical property of the molecules.[18] Molecular packing can be modulated by the non-covalent interaction which is the main strategy to develop the light emitting materials. Various modulation of non-covalent interactions due to the substituent in organic materials are being found such as diphenylbutadienes showed red shifted luminescence in aggregate state when alkyl substituent was present where aromatic C-H•••π, aliphatic C-H•••N and C-H•••π interactions were responsible for molecular packing.[19] Curtis and co-workers remarked the H- and J-aggregate as 'pitch' and 'roll' inclination which are formed by the co-facial π stacked and herringbone π•••π interactions in solid state conjugated oligomers.[20] Using crystal engineering technique, the design strategy could be developed through the non-covalent interactions which could change the molecular conformation with electronic delocalization in molecular packing.[17]

In this chapter, photophysical properties of three new bis(pyridyl)-disulfonamides described. These compounds are analogous to bis(pyridyl)-diamides, where carbon is present in place of sulfur (Scheme 3C.3). Amides are well known for their homomeric synthons and presence of pyridyl groups in bis(pyridyl)-diamides has shown, in some cases, formation of heteromeric

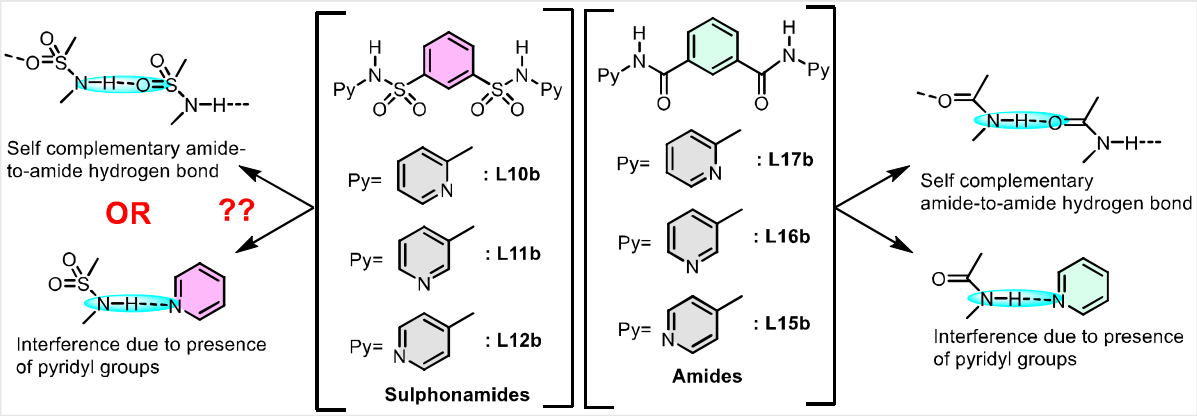

Scheme 3C.3: Bis(pyridyl)-disulfonamides and their amidic counter parts[3]

synthons as well. Crystal structure of **L15b** and **L16b** are reported elsewhere while there is one report of crystal structure of **L17b** where DMF is involved in hydrogen bond interactions with the amide groups.[3] In **L15b** and **L16b**, amide to amide hydrogen bond interactions are interfered due to the presence of pyridyl groups and also because of steric constraints of rigid aromatic spacer. There are many reports involving the coordination complexes of **L15b** and **L16b** where the homomeric synthons of amides are present while in some cases amides are involved in hydrogen bond interactions with solvents.[21] Sang-gi Lee and co-workers have reported the involvement of amide functional groups in **L17b** for capturing a chiral guest molecule through the strong intermolecular hydrogen bonding (N-H···N and N-H···O) interactions and resulted the host-guest molecule, which was further used to synthesize rhodium catalyst for asymmetric hydrogenation.[22]

In this chapter, effect of the presence of sulfur in bis(pyridyl)-disulfonamides on the various possibilities of non-covalent interactions is studied and impact of structural arrangements of these molecules on photophysical properties is analyzed. The structure property correlation was established through the analysis of crystal structure of bis(pyridyl)-disulfonamides.

3C.2 Experimental

3C.2.1 General

^{1}H and ^{13}C NMR spectra were recorded on a Bruker 400 MHZ spectrometer. FTIR spectra were obtained from Shimadzu IRAffinity-1S system. Powder X-Ray Diffraction (XRD) data was collected using a Rigaku miniflex II, λ =1.54 Å, Cu Kα. UV-Visible and fluorescence spectra were recorded on Jasco V-650 spectrophotometer and Fluorimax-4 0426C0809 respectively.

3C.2.2 Single crystal XRD

The single crystal XRD analysis of **L10b** and **L11b** was done at Narendrapur Ramkrishna Mission, Kolkata, using a Bruker AXS D8 QUEST ECO diffractometer equipped with monochromatic Mo-target rotating anode X-ray and graphite monochromator α radiation with λ = 0.71073 Å by ω and φ scan technique. The integrated diffraction data, unit cell and data correction were performed by using Bruker SAINT system, SMART and SADABS respectively. The structure was solved by SHELXS-97 through direct method and refined by full matrix least squares based on F^2 through SHELXS-2018/3.[23] The hydrogen atoms were added at determined positions as riding atoms and non-H atoms were refined anisotropically.

3C.2.3 General procedure for the synthesis of bis(pyridyl)-disulfonamide ligands

Compounds **L10b, L11b** and **L12b** were synthesised following the literature procedure.[24] Aminopyridine was added to disulfonyl dichloride solution in 1,4-dioxane in 1:2 molar ratio and refluxed for 6 hours. The solid residue was washed with cold water and recrystallised from ethanol.

3C.2.3.1 Synthesis of *N*^{1},*N*^{3}-di(pyridin-2-yl)benzene-1,3-disulfonamide (L10b)

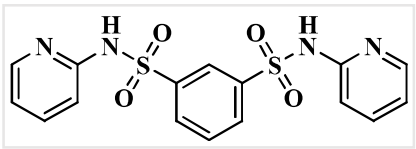

2-Aminopyridine (1.88 g, 20 mmol) was added benzene-1,3-disulfonyl dichloride (2.75 g, 10 mmol) solution in 1,4-dioxane (50 mL) and refluxed for 6 hours. The white solid residue was washed with cold water and recrystallised from ethanol. Yield: 49%; Melting point: (242-244) °C; IR (cm^{-1}): 1670(w), 1624(m), 1531(s), 1462(m), 1381(m), 1357(m), 1130(vs), 956(m),813(s), 682(s), 578(m), 551(m) (Figure A-51); ^{1}H NMR (400 MHz, DMSO-d_6) δ ppm: 12.87 (2H, s, Amide NH), 8.30 (1H, s, ArH), 8.02 (2H, dd, *J* = 7.8, 1.8 Hz, ArH), 7.95 – 7.90 (2H, m, ArH), 7.80 – 7.65 (3H, m, ArH), 7.16 (2H, d, *J* = 8.8 Hz, ArH), 6.84 (2H, t, *J* = 6.5 Hz, ArH) (Figure A-52). ^{13}C NMR (100 MHz, DMSO-d_6) δ ppm: 154.23, 143.81, 142.19, 130.46, 129.84, 124.66, 124.01, 115.01 (Figure A-53).

3C.2.3.2 Synthesis of *N*^{1},*N*^{3}-di(pyridin-3-yl)benzene-1,3-disulfonamide (L11b)

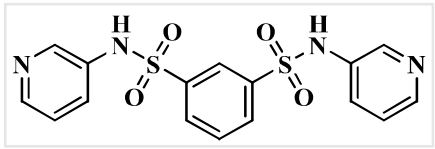

3-Aminopyridine (1.88 g, 20 mmol) was added benzene-1,3-disulfonyl dichloride (2.75 g, 10 mmol) solution in 1,4-dioxane (50 mL) and refluxed for 6 hours. The white solid

residue was washed with cold water and recrystallised from ethanol. Yield: 51%; Melting point: 239-240 °C; IR (cm^{-1}): 1585(m), 1419(m), 1357(m), 1315(m), 1265(m), 1176(m), 1157(vs), 1111(m), 933(vs), 790(s), 682(s), 578(m), 543(vs) (Figure A-54); ^{1}H NMR (400 MHz, DMSO-d_6) δ ppm: 10.82 (2H, s, Amide NH), 8.30 (2H, d, *J* = 4.6 Hz, ArH), 8.26 – 8.20 (2H, m, ArH), 8.14 (1H, t, *J* = 1.9 Hz, ArH), 7.97 (2H, dd, *J* = 7.8, 1.9 Hz, ArH), 7.77 (1H, t, *J* = 7.9 Hz, ArH), 7.41 (2H, dt, *J* = 8.5, 1.9 Hz, ArH), 7.28 (2H, dd, *J* = 8.3, 4.7 Hz, ArH) (Figure A-55); ^{13}C NMR (100 MHz, DMSO-d_6) δ ppm:146.23, 142.58, 140.58, 134.14, 131.75, 131.52, 128.60, 125.29, 124.59 (Figure A-56).

3C.2.3.3 Synthesis of *N*^{1},*N*^{3}-di(pyridin-4-yl)benzene-1,3-disulfonamide (L12b)

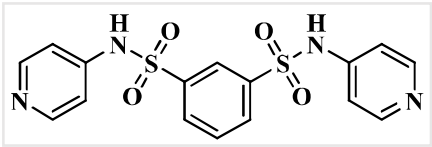

4-Aminopyridine (1.88 g, 20 mmol) was added benzene-1,3-disulfonyl dichloride (2.75 g, 10 mmol) solution in 1,4-dioxane (50 mL) and refluxed for 6 hours. The white solid residue was washed with cold water and recrystallised from ethanol. Yield: 54%; Melting point: 152-155 °C; IR (cm^{-1}): 1635(m), 1489(vs), 1346(s), 1257(m), 1157(m), 1091(vs), 999(w), 802(vs), 783(vs), 759(s), 686(m), 586(m), 551(m) (Figure A-57); ^{1}H NMR (400 MHz, DMSO-d_6) δ ppm: 12.79 (2H, s, Amide NH), 8.15 (1H, t, *J* = 1.8 Hz, ArH), 8.05 – 7.98 (4H, m, ArH), 7.93 (2H, dd, *J* = 7.8, 1.8 Hz, ArH), 7.63 (1H, t, *J* = 7.8 Hz, ArH), 6.96 – 6.90 (4H, m, ArH).(Figure A-58); ^{13}C NMR (100 MHz, DMSO-d_6) δ ppm: 144.73, 139.95, 130.09, 129.01, 123.82, 115.19 (Figure A-59); HRMS: m/z calcd for $C_{16}H_{14}N_4O_4S_2$ $(M+H)^+$ = 391.0529, found 391.0519 (Figure A-60).

3C.3 Results and discussion

Three new bis(pyridyl)-disulfonamide compounds (**L10b**-**L12b)** were synthesized and out of them, molecular structures of **L10b** and **L11b** were established using single crystal XRD studies (Table 3C.1). Photophysical properties of these compounds also showed interesting observations which were correlated with their solid-state structures. The pyridyl nitrogen has played a vital role in controlling the ACQ to AIEE properties. **L10b** and **L12b** having 2/4-pyridyl rings showed the ACQ in solid state as well as at higher concentration while **L11b** containing 3-pyridyl rings showed AIEE at higher concentration. Further the amidic analogues **L15b**[3b], **L16b** and **L17b**[3a] whose structures reported elsewhere were compared and analyzed to understand the effect of different geometrical and electronic centres in amides and sulfonamides on the overall supramolecular arrangement of the molecules (Scheme 3C.1).

Table 3C.1: Crystallographic data of **L10b**, and **L11b**

	L10b	**L11b**
Chemical formula	$C_{16}H_{14}N_4O_4S_2$	$C_{16}H_{14}N_4O_4S_2$
Formula weight	390.43	390.43
Temperature (K)	297(2)	293(2)
Wavelength (Å)	0.71073	0.71073
Crystal system	Monoclinic	Orthorhombic
Space group	*C2/c*	$P\,2_12_12_1$
a (Å)	17.7885(9)	9.3978(5)
b (Å)	9.7086(4)	9.6887(5)
c (Å)	9.5753(4)	19.6049(11)
α (°)	90	90
β (°)	100.825(4)	90
γ (°)	90	90
Z	4	4
Volume (Å^3)	1624.24(13)	1785.07(17)
Density (g/cm^3)	1.597	1.453
μ (mm^{-1})	0.361	0.328
Theta range	3.083° to 24.729°	2.345° to 28.250°
F(000)	1760	2556
Reflections collected	5708	28332
Independent reflection	1375	4409
Reflections with I >2σ(I)	1218	4209
R_{int}	0.0316	0.0418
Number of parameters	123	235
GO F on F^2	1.073	1.046
Final $R_1{}^a/wR_2{}^b$ (I >2σ(I))	0.0873	0.037
Largest diff. peak and hole (eÅ^{-3})	0.665 & -0.627	0.225 & -0.435

[a] $R_1 = \sum||F_o| - |F_c||/\sum|F_o|$. [b] $wR_2 = [\sum w(F_o^2 - F_c^2)^2/\sum w(F_o^2)^2]^{1/2}$, where $w = 1/[\sigma^2(F_o^2) + (aP)^2 + bP]$, $P = (F_o^2 + 2F_c^2)/3$.

3C.3.1 Crystal structure analysis of L10b

The crystal structure analysis of **L10b** revealed that it has crystalized in *C*2/c space group and half of the molecule is present in the asymmetric unit (Figure 3C.3). Presence of three aromatic ring systems in the molecule provided rigidity while the tetrahedral sulfur centre dictated an overall non-planar geometry of the molecule. The pyridyl ring plane is oriented almost perpendicular to the central phenylene

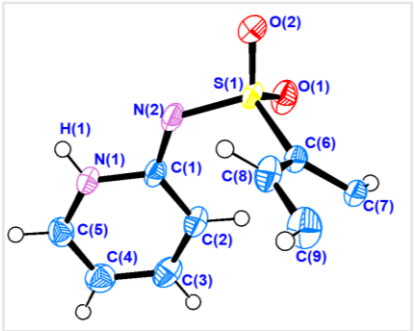

Figure 3C.3: ORTEP (showing thermal ellipsoid at 50% probability) of asymmetric unit of **L10b**

ring plane, while the angle between the two pyridyl rings of the molecule is about 58° (Figure 3C.4a). The torsion angles H1-N1-C1-N2 (7.14°), C1-N2-S1-O2 (177.80°) and C1-N2-S1-O1 (48.50°) clearly shows that geometrically the proton on pyridyl ring nitrogen and one of the sulfone oxygens are in one plane and can have favourable bifurcated hydrogen bond interactions (N-H···N and NH···O) with another molecule of L10b. It was observed from the crystal structure that N-H···N hydrogen bond (2.131 Å, H1-N2) is stronger than NH···O hydrogen bond (2.538 Å, H1-O2) due to the positioning of nitrogen atom in the pyridyl ring. The N-H···N hydrogen bonds between the molecules of **L10b** resulted in the formation of 1D chains (Figure 3C.4b). The stacking of those hydrogen bonded 1D chains occurred via aromatic interactions between the pyridyl groups of the adjacent chains and also via weak C-H···O type interactions between the phenylene groups and the oxygen of the sulfonamides (Figure 3C.4c).

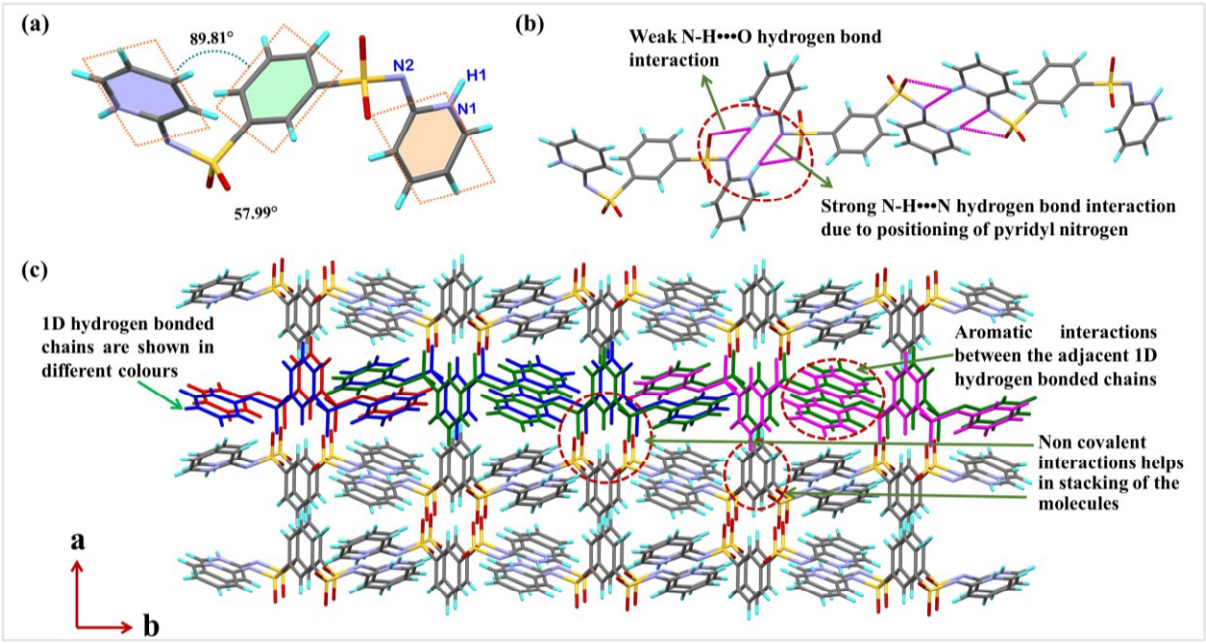

Figure 3C.4: Illustrations of crystal structure of **L10b**: (a) Geometry of a molecule of **L10b**; (b) N-H···N hydrogen bonded interactions resulting in 1D hydrogen bonded chains; (c) packing of the molecules via various non-covalent interactions

3C.3.2 Crystal structure analysis of L11b

L11b molecules has crystallized in orthorhombic $P2_12_12_1$ and one molecule of **L11b** is present in the asymmetric unit (Figure 3C.5). Geometry of the molecule of **L11b** showed that two pyridyl ring planes are oriented at angles 77.87° and

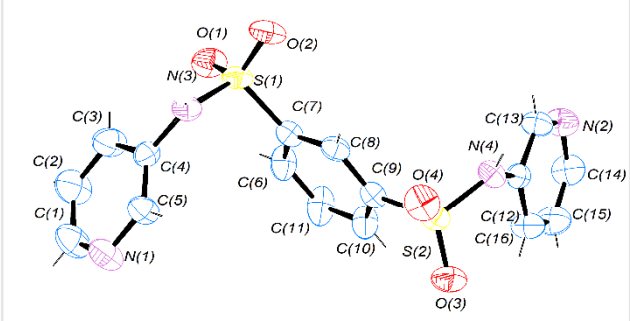

Figure 3C.5: ORTEP (showing thermal ellipsoid at 50% probability) of asymmetric unit of **L11b**

60.40° with phenylene ring plane while the two pyridyl ring planes are making an angle 76.95° (Figure 3C.6a). Presence of N-H···N hydrogen bond interactions resulted overall packing of the **L11b** molecules in crystal structure (Figure 3C.6b). It should be noted that due to the presence of 3-pyridyl ring in **L11b**, the hydrogen bond interactions of the pyridyl nitrogen atom and amidic nitrogen atom do not lead to the formation of the cyclic ring structure as in **L10b** (Figure 3C.4b). Moreover, each molecule of **L11b** interacts with four different **L11b** molecules via N-H···N hydrogen bond interactions (Figure 3C.6c). The rigidity of the aromatic rings and scope of obtaining stability due to hydrogen bond interactions has resulted in overall bent and highly non-planar geometry of the **L11b** molecules.

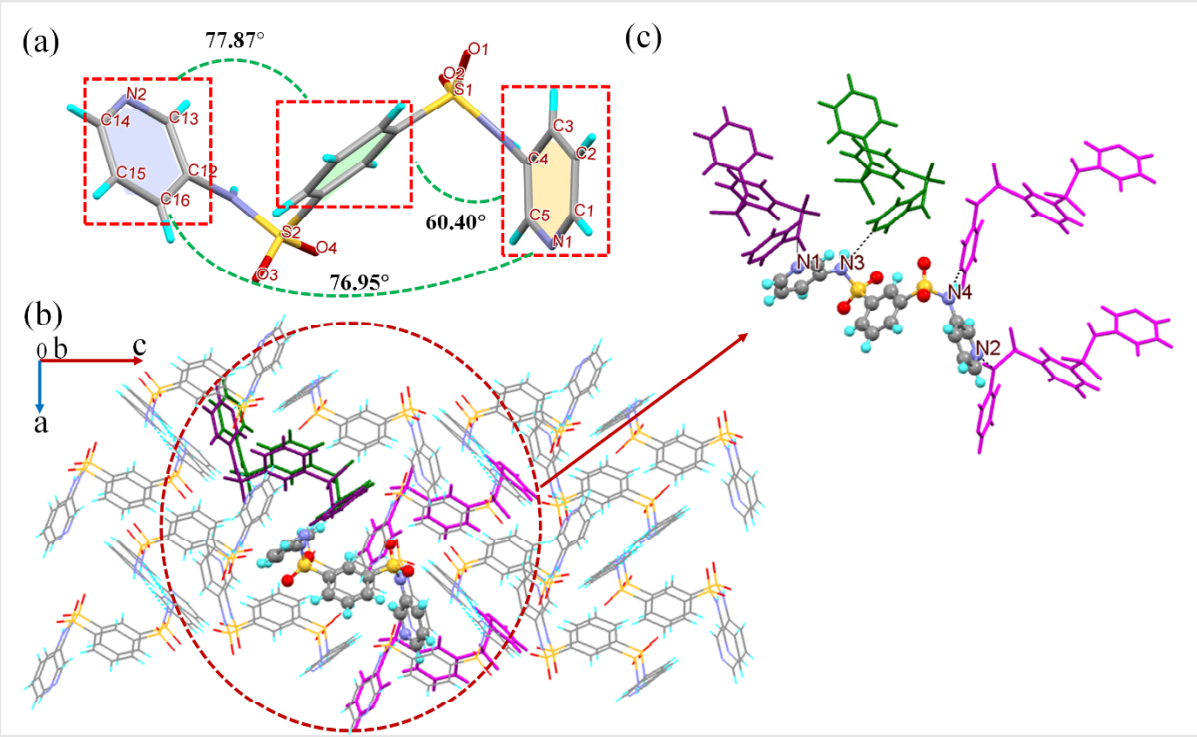

Figure 3C.6: Illustrations of crystal structure of **L11b**: (a) Geometry of a molecule of **L11b**; (b) N-H···N hydrogen bonded interactions resulting packing of **L11b**; (c) N-H···N hydrogen bonded interactions between the **L11b** molecules

3C.3.3 Powder XRD of the L10b and L11b

Powder XRD spectra were taken for **L10b** and **L11b** and compared with simulated powder XRD which is generated from the single-crystal X-ray data. Figure 3C.7 shows the phase purity of the **L10b** and **L11b**.

3C.3.4 Comparison of crystal structure of sulfonamides with their amidic analogues

Crystal structure of the amidic counter parts of **L10b** (**L17b**), **L11b** (**L16b**) and **L12b** (**L15b**) are reported elsewhere.[3b, 25] The presence of trigonal planar carbon centre in those compounds

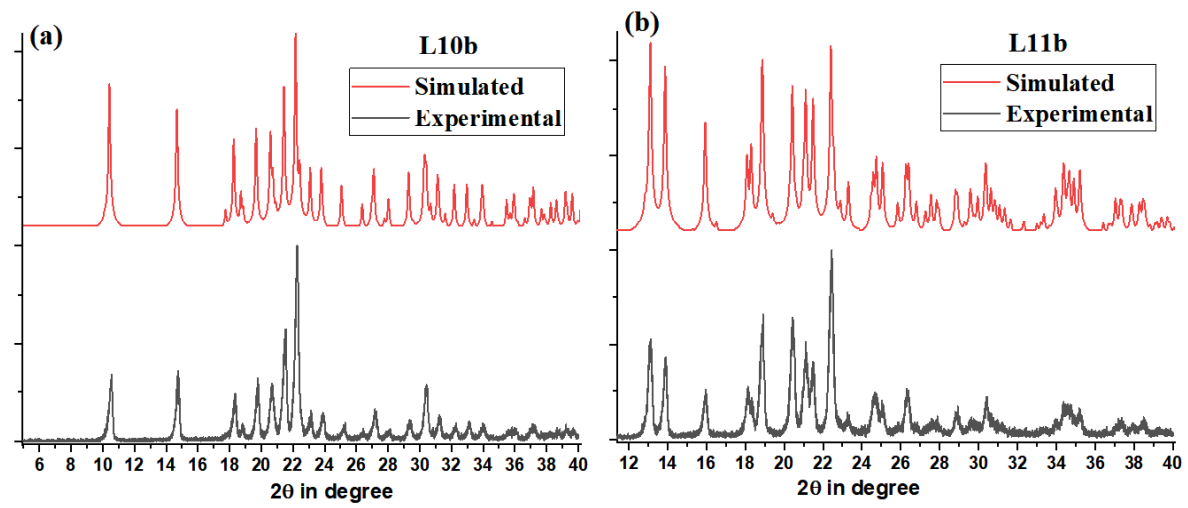

Figure 3C.7: (a) Experimental and simulated powder XRD of **L10b**; (b) Experimental and simulated powder XRD of **L11b**

in place of tetrahedral sulfur centre in **L11b** and **L12b** has effected overall crystal packing. In case of **L11b**, the presence of sulfur centre and 3-pyridyl group has resulted in non-planar molecular geometry (Figure 3C.6a), while in its amidic analogue, the planar amide functional group has provided enough opportunity for the molecule to sustain a relatively planar geometry (Figure 3C.8a). The hydrogen bond interactions between the molecules in the amidic analogue (**L16b**) has formed a 1D network, while the directionality of the N-H•••N hydrogen bond interactions in **L11b** is dictated by the non-planarity of the molecules and gave a final 3D hydrogen bonded network for **L11b** (Scheme 3C.4). Crystal structure of **L12b** is not determined. Its amidic analogue (**L15b)** showed the formation of a 2D hydrogen bonded

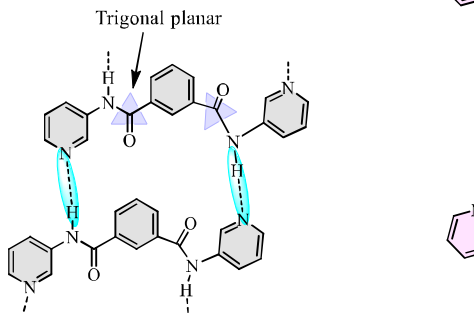

(i) More symmetric molecular geometry than the sulfonamide analogue
(ii) Rigidity of the aromatic groups and 1,3-substituted central phenyl ring has prevented the self complimentary amide-to-amide bonds (N-H•••O) in both the compounds

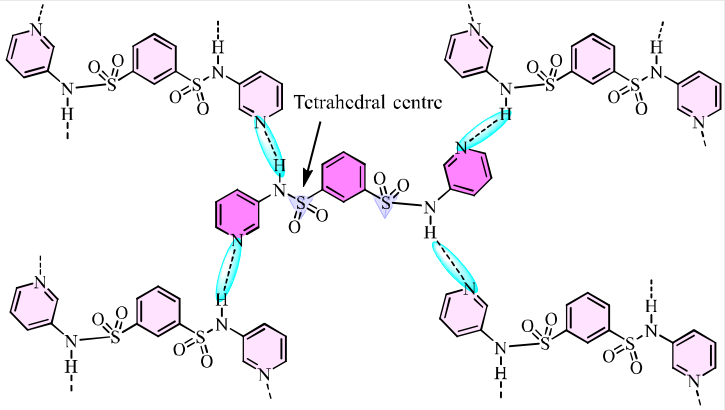

(iii) Tetrahedral sulfur centre in **L11b** has incorporated more non planarity in the molecule. So the N-H•••N hydrogen bonded network is extending along 3D
(iv) Trigonal planar carbon centre has induced relatively planar molecular geometry and the resulting N-H•••N hydrogen bonded network is a 1D chain

Scheme 3C.4: (a) Arrangement of the molecules of **L16b**; notice the prevention of self-complimentary amide to amide hydrogen bonds, (b) arrangement of the molecules of **L11b**; notice the formation of N-H-N hydrogen bond due to tetrahedral sulfur centre

network via N-H•••N hydrogen bond interactions (Figure 3C.9). The amidic analogue (**L17b**) of **L10b** is reported where a solvent molecule is present in the structure, which interfered with the hydrogen bond interactions within the molecules.[3a] Hence analysis of the structural similarities of **L10b** with its amidic counterpart cannot be verified appropriately.

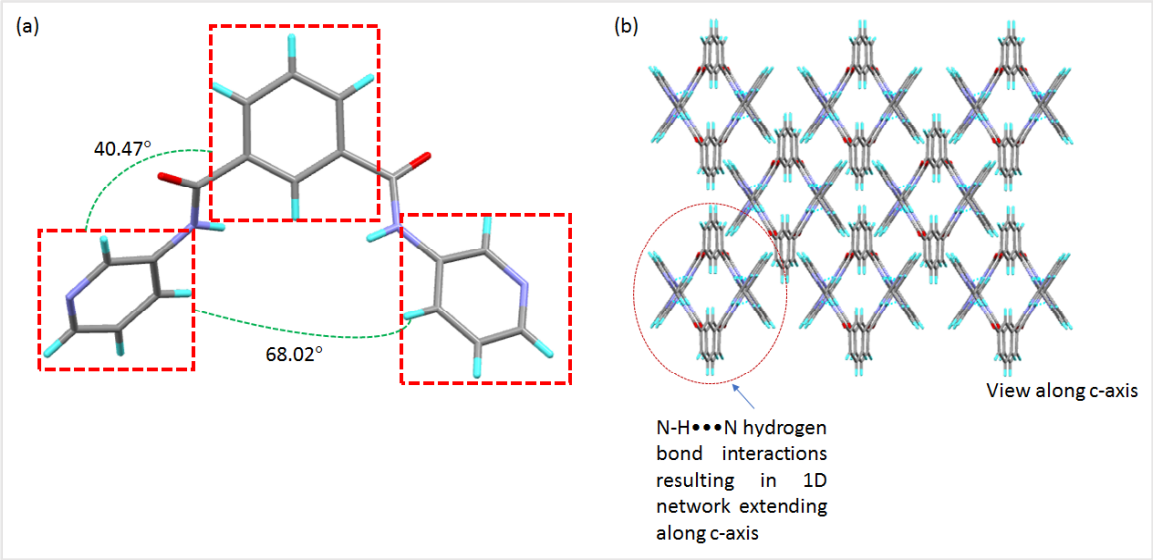

Figure 3C.8: Illustrations of crystal structure of **L16b**: (a) Molecular geometry (b) packing of molecules via N–H•••N hydrogen bond interactions to form 1D network; Structures are generated from CCDC no. 259256

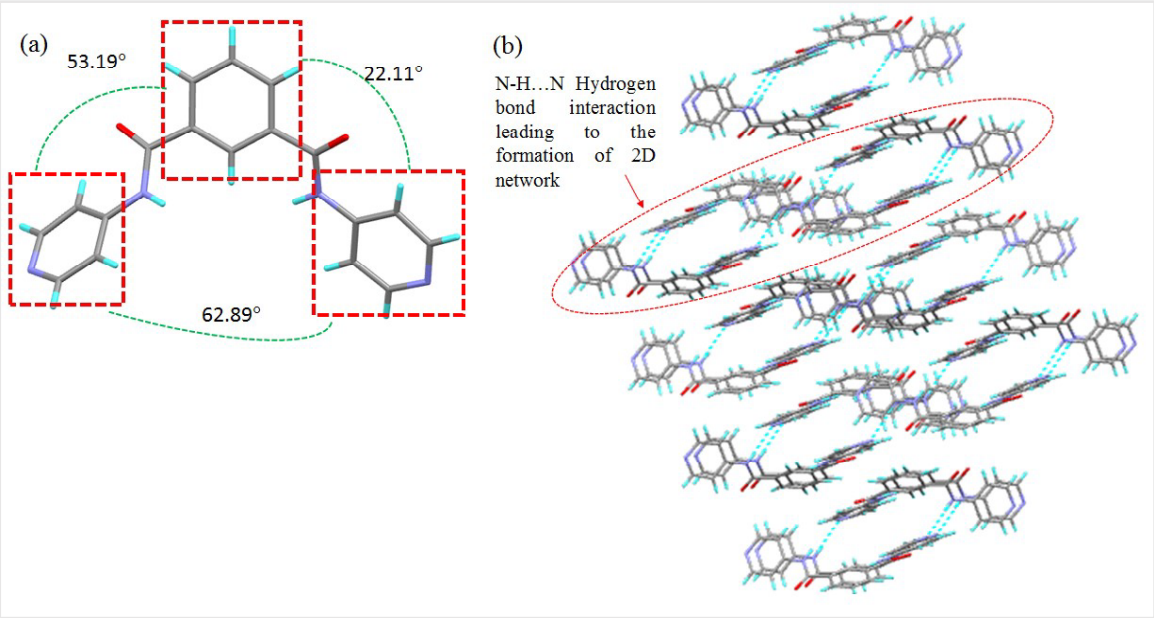

Figure 3C.9: Illustrations of crystal structure of **L15b**: (a) Molecular geometry (b) packing of molecules via N–H•••N hydrogen bond interactions to form 2D network; Structures are generated from CCDC no. 694503

3C.3.5 UV-Visible absorption studies

UV-Visible absorption spectra of **L10b**-**L12b** were recorded by dissolving the compounds in methanol for the solution-state spectral analysis, while for the solid-state spectral analysis, the compounds were mixed with $BaSO_4$. UV-Visible absorption spectrum of **L10b** showed two

major peaks (λ_{max} = 241 nm and λ_{max} = 317 nm) when taken in methanol and also showed similar peak positions (250 nm and 314 nm) in solid state (Figure 3C.10a & Table 3C.2). Similarly, **L12b** resulted in a peak at wavelength 293 nm when taken in methanol, while the solid state spectra showed peaks at 260 nm, 308 nm and 372 nm (Figure 3C.10c). When compared with **L10b** and **L12b**, a completely different UV-visible absorption spectrum was observed in the case of **L11b** due to the presence of 3-pyridyl ring (Figure 3C.10b). In solution state, **L11b** showed absorption maxima at wavelengths 247 nm and 276 nm. It is observed from the UV-Visible spectra that n $\rightarrow$ * transitions in **L11b** (276 nm) is blue shifted as compared to that in **L10b** (317 nm) and **L12b** (293 nm). The blue shift of this transition in **L11b** can be attributed both to the electronic as well as geometrical factors. Crystal structure of **L11b** showed a highly nonplanar molecular geometry which resulted in blue shift of absorption peak position as compared to **L10b.**

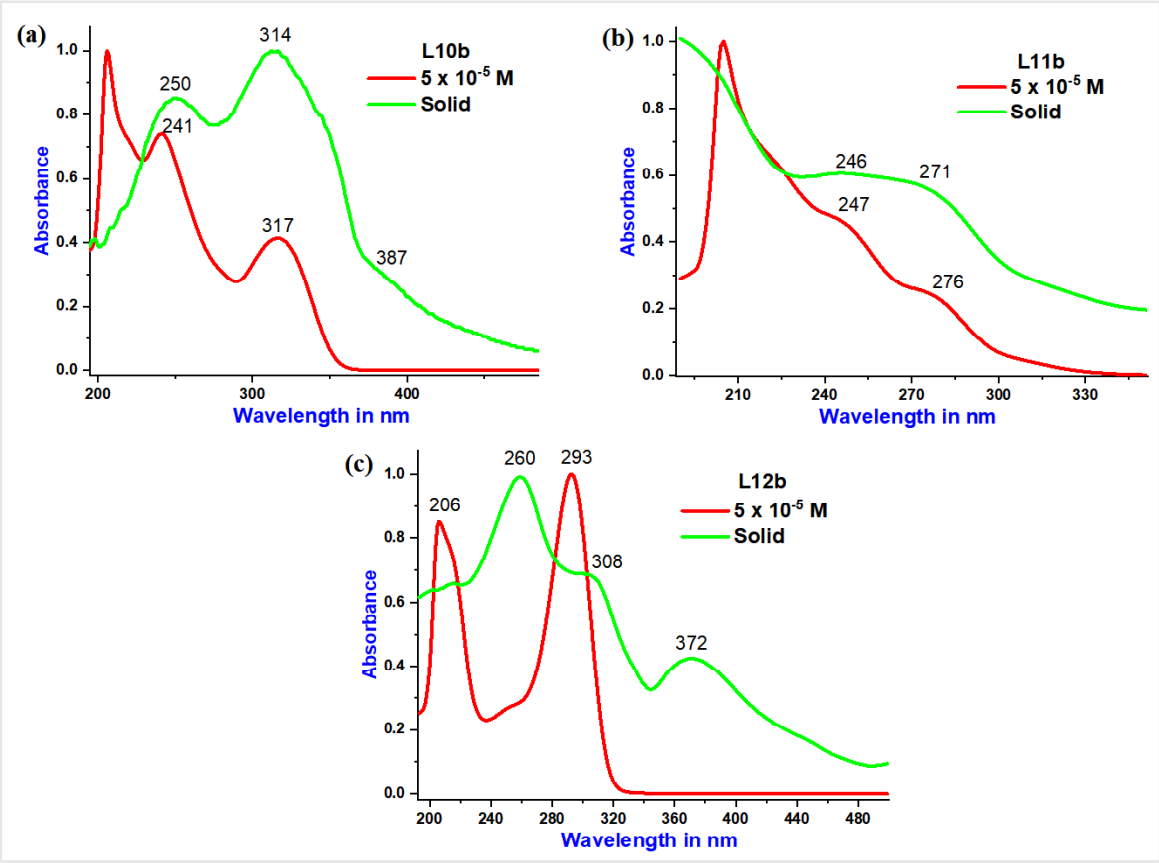

Figure 3C.10: UV-Visible spectra of **L10b**-**L12b** in methanol and solid state: (a) **L10b** (b) **L11b** and (c) **L12b**

Table 3C.2: Comparison of λ_{max} values of solution and solid state spectra

Compound	Solution	Solid
L10b	241, 317	250, 314
L11b	247, 276	246, 271
L12b	206, 293	260, 308, 372

3C.3.6 Emission spectra of L10b-L12b

The compounds **L10b**-**L12b** are non-emissive in solid state. The emission spectra of these compounds were recorded in methanolic solution at room temperature, where an increase in the intensity of photoluminescence was observed on gradually decreasing the concentration of **L10b** and **L12b**. At an excitation wavelength of 317 nm, **L10b** showed a maximum intensity for 1×10^{-4} M solution (Figure 3C.11a). In case of **L12b**, at excitation 260 nm, maximum emission was observed for 1×10^{-6} M solution (Figure 3C.11c). In case of **L11b**, concentration-dependent emission spectra showed an opposite trend compared to that in **L10b** and **L12b**. At an excitation wavelength 300 nm, increase in the intensity of photoluminescence spectra is observed on increasing the concentration of **L11b** (Figure 3C.11b). For **L10b** and **L12b**, aggregation caused quenching (ACQ) was observed, while for **L11b**, although the solid-state compound did not show any emission, aggregation induced emission (AIE) was observed in solution state.

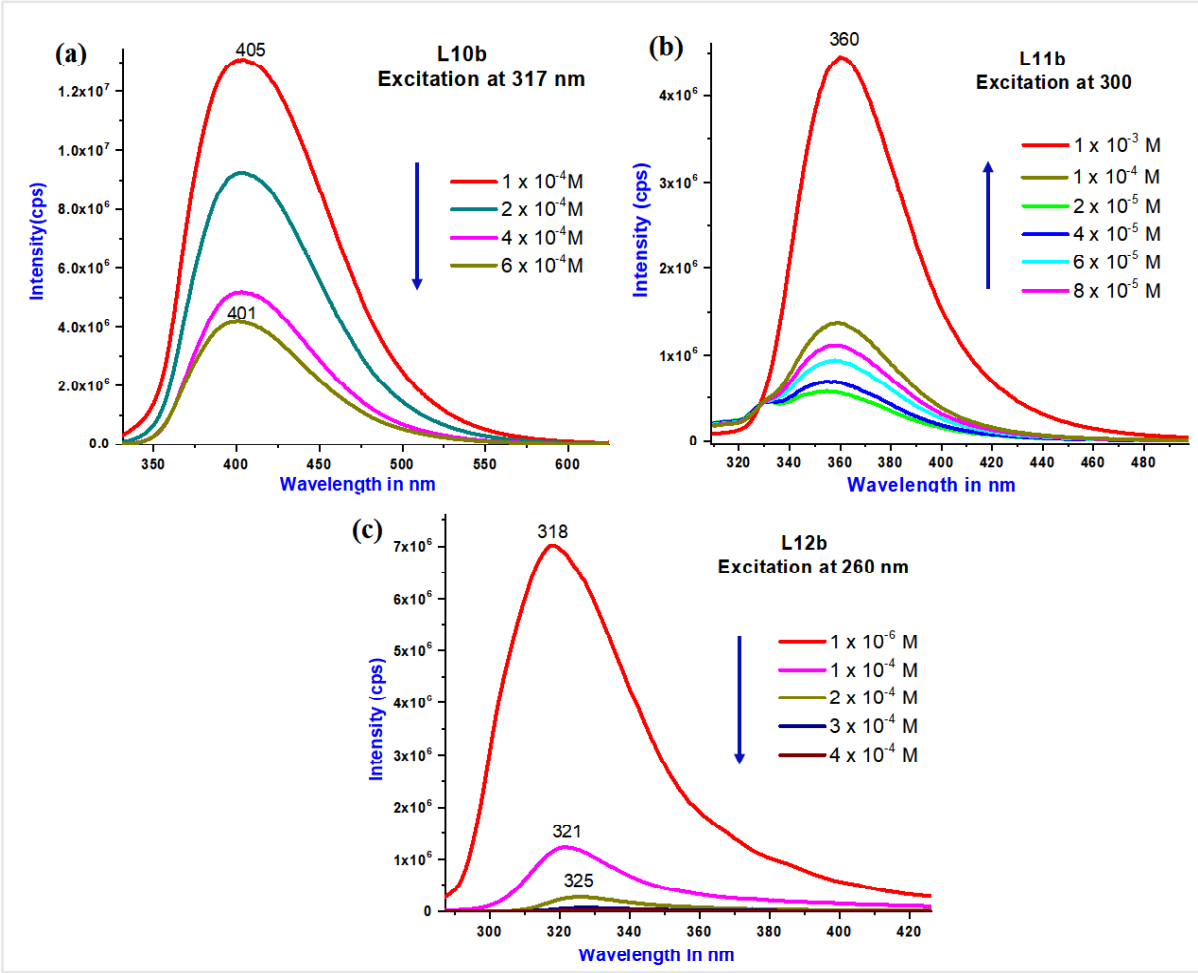

Figure 3C.11: Concentration dependent emission spectra: (a) **L10b**; (b) **L11b** and (c) **L12b**

Non-emissive nature of **L10b** and **L11b** in the solid state can be rationalized based on their crystal structure. The crystal structure of **L10b** showed the packing of the molecules via aromatic interactions along with other non-covalent interactions. Quenching of photoluminescence in solid **L10b** may be associated with the stacking of the aromatic planes. In **L11b**, the position of the nitrogen atom in the 3-pyridyl group and the tetrahedral sulfur centre has resulted in loss of planarity of the molecule in solid state, which might be associated with the non-emissive nature of **L11b** in solid state. The crystal structure of **L12b** is not determined but the optimized structure showed a relatively planar geometry of the molecule. Hence the non-emissive nature of **L12b** in the solid state may be attributed to the reasons similar to that of **L10b**, that is the stacking of aromatic moieties (Scheme 3C.5). In solution state, ACQ showed by **L10b** and **L12b** is associated with deactivation of excited state due to stacking of aromatic rings. In **L11b**, AIE was observed in solution state as rigidity associated with the solid state and hence the non-planar geometry is relaxed, leading to emission in the solution. In solution state, increase in concentration of **L11b** resulted in the increase of photoluminescence intensity as the geometrical features of the compound prevents the molecules from stacking at higher concentrations, which does not allow ACQ (Scheme 3C.5).

3C.4 Conclusion

Sulfonamides are explored widely in medicinal chemistry and derivatives of disulfonamide have also been reported in this field. There are very few reports on mono sulfonamides having photophysical applications. According to our knowledge, this is the first study of analyzing photophysical properties of disulfonamides. Inspired by the electronic structure of bis(pyridyl)-diamides, tuning the nitrogen in the pyridyl ring to *ortho*, *para*, and *meta* positions, three new bis(pyridyl)-disulfonamides were synthesized and their photophysical properties were studied which is decided by the rationale interplay of the relation between the geometry and non-covalent interactions. It is found that for **L10b** (2-pyridyl) and **L12b** (4-pyridyl), ACQ was observed at higher concentration and were emissive in nature at very low concentration. Quenching in the intensity of PL in the case of all sulfonamides was observed in solid state due to their face-to-face stacking of aromatic rings. The introduction of 3-pyridyl ring, and the tetrahedral sulfur centre in **L11b** made the unique geometry which helped to rearrange the molecules to turn ACQ into AIE in solution state.

(a) 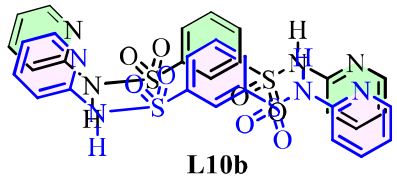

L10b

Aromatic stacking in solid state structure

(c) 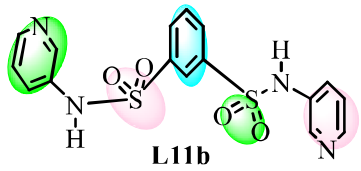

L11b

Non planar molecular geometry in solid state structure

(b) 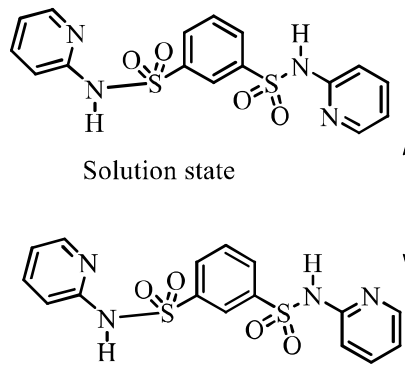

Solution state

Molecules of **L10b** are far apart in dilute solutions, so aromatic stacking is prevent and dilute solutions becomes emissive, while ACQ is observed at higher concentration

(d) 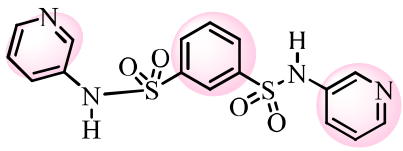

In solution state, the hydrogen bond interactions between the molecules will be relaxed due to increase in distance between the molecules and hence the molecular rigidness can be relaxed and the moelcule can attain some sort of planarity.

As stacking is avoided in solution state, so ACQ is not observed the solution state for **L11b**.

Scheme 3C.5: Arrangement of the molecules of **L10b** in solid state and in solution state (a) & (b); observe face to face stacking in solid state (a); notice the prevention of ACQ in lower concentration (b), no fluorescence observe in solid state due to non-planarity (c); non-planarity of **L11b** diminished in solution state (d)

3C.5 References

[1] (a) Ema T., Okuda K., Watanabe S., Yamasaki T., Minami T., Esipenko N. A., Anzenbacher P., *Org. Lett.,* **2014**, 16(5), 1302-1305; (b) Wienkers M., Ramos J., Jemal H., Cardenas C., Wiget P., Nelson A., Free S., Wu J., Roach R., Vulcan M., Waynant K., Fort K., Vladimirova A., Sun J., Hunt S. E., Rudkevich D. M., Starnes S. D., *Org. Lett.,* **2012**, 14(6), 1370-1373.

[2] (a) Sarkar M., Biradha K., *Chem. Commun.,* **2005**, 2005(17), 2229-2231; (b) Sarkar M., Biradha K., *Cryst. Growth Des.,* **2006**, 6(1), 202-208; (c) Sarkar M., Biradha K., *Cryst. Growth Des.,* **2007**, 7(7), 1318-1331; (d) Chourasiya S. S., Patel D. R., Nagaraja C. M., Chakraborti A. K., Bharatam P. V., *New J. Chem.,* **2017**, 41(16), 8118-8129; (e) Zhang S., Zhang Y., Wang C., Zhu R., *Acta Crystallogr. Sect. Sect. E: Struct. Rep. Online,* **2011**, 67(11), o2831-o2831.

[3] (a) Qin D.-B., Jin L.-H., Gu S.-J., *Acta Crystallogr. Sect. Sect. E: Struct. Rep. Online,* **2006**, 62(10), o4519-o4520; (b) Adarsh N. N., Kumar D. K., Dastidar P., *CrystEngComm,* **2009**, 11(5), 796-802; (c) Yue N. L. S., Eisler D. J., Jennings M. C., Puddephatt R. J., *Inorg. Chem.,* **2004**, 43(24), 7671-7681.

[4] Thapa K. B., Chen J.-D., *CrystEngComm,* **2015**, 17(25), 4611-4626.

[5] Rodrigues V. Z., Foro S., Gowda B. T., Shakuntala K., *Acta Crystallogr. Sect. Sect. E: Struct. Rep. Online,* **2011**, 67(11), o3040-o3040.

[6] Yousef F., Mansour O., Herbali J., *In-vitro In-vivo In-silico Journal,* **2018**, 1(1), 1.

[7] Sonu, Parveen B. R., Praveen S., Pal H., *Int. J. Pharm. Chem.,* **2017**, 7(5), 70-73.

[8] Singh S., Chawla P., Chawla V., Saraf S. K., *Rasayan J. Chem.,* **2013**, 6(3), 196-200.

[9] Greed S., Briggs E. L., Idiris F. I. M., White A. J. P., Lücking U., Bull J. A., *Chem. Eur. J.,* **2020**, 26(55), 12533-12538.

[10] Wang H., Liang Y., Xie H., Feng L., Lu H., Feng S., *J. Mater. Chem. C,* **2014**, 2(28), 5601-5606.

[11] Liu Y., Tao X., Wang F., Shi J., Sun J., Yu W., Ren Y., Zou D., Jiang M., *J. Phys. Chem. C,* **2007**, 111(17), 6544-6549.

[12] (a) Kuś P., Kusz J., Książek M., *J. Chem. Crystallogr.,* **2020**, 50(1), 21-27; (b) Nishio M., *CrystEngComm,* **2004**, 6(27), 130-158.

[13] Zakerhamidi M. S., Ahmadi-Kandjani S., Moghadam M., Ortyl E., Kucharski S., *J. Mol. Struct.,* **2011**, 996(1), 95-100.

[14] Bozkurt E., Gul H. İ., Tugrak M., *Turk. J. Chem.,* **2017**, 41(2), 282-293.

[15] Zakerhamidi M. S., Ahmadi-Kandjani S., Moghadam M., Ortyl E., Kucharski S., *Spectrochim. Acta, Part A,* **2012**, 85(1), 105-110.

[16] Baig F., Kant R., Gupta V. K., Sarkar M., *RSC Adv.,* **2015**, 5(63), 51220-51232.

[17] Varughese S., *J. Mater. Chem. C,* **2014**, 2(18), 3499-3516.

[18] Das M., Baig F., Sarkar M., *RSC Adv.,* **2016**, 6(63), 57780-57792.

[19] Davis R., Saleesh Kumar N. S., Abraham S., Suresh C. H., Rath N. P., Tamaoki N., Das S., *J. Phys. Chem. C,* **2008**, 112(6), 2137-2146.

[20] Curtis M. D., Cao J., Kampf J. W., *J. Am. Chem. Soc.,* **2004**, 126(13), 4318-4328.

[21] (a) Das M., Khullar S., Sarkar M., *Eur. J. Inorg. Chem.,* **2020**, 2020(33), 3174-3186; (b) Sarkar M., Biradha K., *Cryst. Growth Des.,* **2006**, 6(8), 1742-1745.

[22] Park J. H., Shin H., Park D. H., Lee S.-g., *Bull. Korean Chem. Soc.,* **2010**, 31(3), 635-638.

[23] Sheldrick G. M., *Acta Crystallogr., Sect. C: Struct. Chem.,* **2015**, 71(1), 3-8.

[24] Shams N., Donia S., ELRAHMAN T. A., *J. Chem. Soc. Pak.,* **1986**, 8(2), 209-216.

[25] Qin Z., Jennings M. C., Puddephatt R. J., *Chem. Eur. J.,* **2002**, 8(3), 735-738.